NANO LETTERS

LETTER

pubs.acs.org/NanoLett

Direct Imprinting of Porous Substrates: A Rapid and Low-Cost Approach for Patterning Porous Nanomaterials

Judson D. Ryckman,[†] Marco Liscidini,[‡] J. E. Sipe,[§] and S. M. Weiss*[,†]

[†] Department of Electrical Engineering and Computer Science, Vanderbilt University, Nashville, Tennessee 37235

[‡] Dipartimento di Fisica "A. Volta", Università degli Studi di Pavia, via Bassi 6, 27100 Pavia, Italy

[§] Department of Physics and Institute for Optical Sciences, University of Toronto, 60 St. George St. Toronto M5S 1A7 Ontario, Canada

Supporting Information

ABSTRACT: This work describes a technique for one-step, direct patterning of porous nanomaterials, including insulators, semiconductors, and metals without the need for intermediate polymer processing or dry etching steps. Our process, which we call "direct imprinting of porous substrates (DIPS)", utilizes reusable stamps with micro- and nanoscale features that are applied directly to a porous material to selectively compress or crush the porous network. The stamp pattern is transferred to the porous material with high fidelity, vertical resolution below 5 nm, and lateral resolution below 100 nm. The process is performed in less than one minute at room temperature and at standard atmospheric pressure. We have demonstrated structures ranging from subwavelength optical components to microparticles and present exciting avenues for applications including surface-enhanced Raman spectroscopy (SERS), label-free biosensors, and drug delivery.

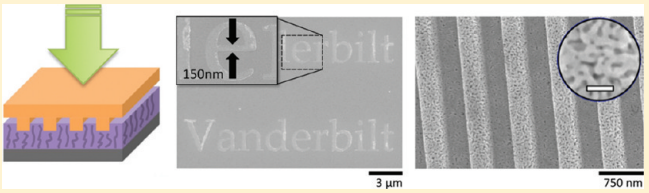

KEYWORDS: Nanoimprinting, porous nanomaterials, photonic structures, sensing, nanofabrication

Porous nanomaterials such as porous silicon (pSi), porous alumina (pAl_2O_3), nanoporous gold (np-Au), and titanium dioxide nanotube arrays (TiO_2-NTAs) are characterized by nanoscale voids and high specific surface area that give rise to their unique optical, electrical, chemical, and mechanical properties. The formation of such porous nanomaterials is self-organizing and elaborate fabrication techniques are not required.[1−5] This results in a class of nanomaterials that is cost-effective to produce and exhibits highly desirable physical and chemical attributes over very large areas ($\sim cm^2$). The challenge in implementing porous materials for a variety of applications, including drug delivery and imaging,[6−8] chemical and biological sensing,[9−12] catalysis,[13−15] biomaterials,[16,17] battery anodes,[18,19] plasmonics,[20] integrated optoelectronics,[21,22] and solar energy conversion,[23−25] is the need to perform micro- and nanometer scale structuring of these materials. The structures and patterns that are required for these applications generally fall into one or more of the following three categories: (i) macro- to microscale arrays (e.g., multiplexed or replicated structures and sensors), (ii) microscale structures (e.g., microparticles), and (iii) submicrometer to nanoscale elements (e.g., subwavelength optical components and nanoparticles).

While many of these structures can be realized through the application of traditional lithography strategies (e.g., electron-beam lithography (EBL) and photolithography), such techniques are expensive and limited by a trade-off between resolution and throughput. The development of nanoimprint lithography (NIL) and soft lithography strategies has enabled high throughput fabrication of nano- to microscale features.[26−29] However, there remain several key challenges associated with applying any of the currently available fabrication techniques to porous nanomaterials. First, resists and thermoplastics are likely to infiltrate the pores, potentially modifying the internal porous structure and often proving very difficult to remove, especially in deep porous networks. Second, for porous materials wet etching is not always an option due to chemical incompatibilities, and dry-etching techniques are expensive and require specific chemistries that must be appropriately characterized and tailored for each unique porous material. Additionally, resists and developers are costly, require complex and time-consuming thermal processing, and generate large quantities of hazardous waste.

New technologies for direct patterning overcome many of the aforementioned challenges by eliminating the need for intermediate masking materials and etch recipes. For example, ultrafast liquefaction has been utilized to achieve direct imprinting of nanoscale features into Si substrates.[30] More recently, indentation lithography has been applied to directly produce topographic patterns on epoxy, Si, and SiO_2.[31] Here, we demonstrate a direct patterning technique specifically motivated for structuring porous nanomaterials. The process can be performed at room temperature in less than one minute. Our technique is based on the concept that a heterogeneous void network can accommodate volume changes in ways that would be impossible for a bulk solid. By applying a premastered stamp to selectively compress or

Received: August 9, 2010
Revised: September 3, 2010
Published: September 17, 2010

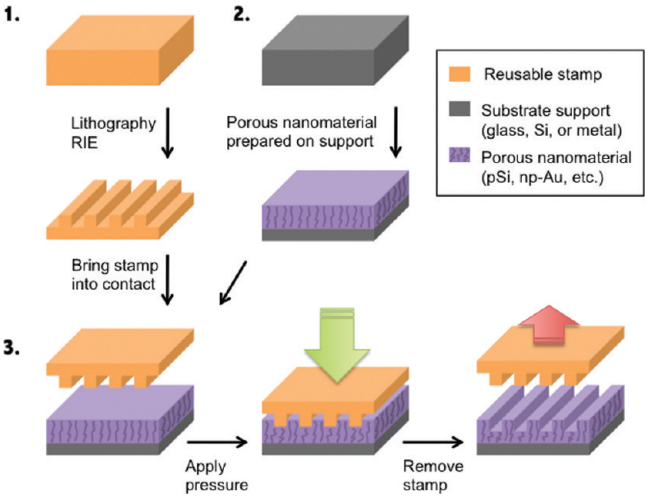

Figure 1. Illustration of DIPS. A reusable stamp is patterned by standard lithography and reactive-ion-etching. The porous material is prepared on a substrate (e.g., silicon, glass, or metal). The stamp is then imprinted into the porous material using an applied pressure on the order of 100 N/mm^2. The stamp is then removed from the substrate, revealing the desired structure. Further device processing of the patterned material can then be performed.

crush localized regions of the underlying porous nanomaterial, direct imprinting of porous substrates (DIPS) not only circumvents the challenges posed by traditional lithographic strategies, but it also allows local manipulation of the internal porous network (e.g., pore size and porosity) and the generation of complex three-dimensional topographies.

Figure 1 illustrates the DIPS process. A porous nanomaterial is prepared on a solid substrate support, for example silicon, glass, or metal, and is subsequently imprinted with a premastered and reusable stamp utilizing an applied pressure $\approx$ 100 N/mm^2 = 100 MPa (approximately 10^3 atm). The straightforward process can be performed in a matter of seconds at room temperature without the need for any curing, developing, baking, or etching processes. In our present investigations, we utilize Si as the stamp material. Silicon stamps with a large variety of imprintable patterns can be readily fabricated through conventional lithographic techniques, and Si has a desirably large material hardness ($\sim$10 GPa). While silicon may not prove to be the optimal choice for a stamp material for all applications,[28] our investigations have demonstrated its potential for extensive reusability and high fidelity imprinting of many porous materials.

As an example of DIPS, Figure 2a shows the imprinting behavior of an $\sim$1 μm thick pSi film with pore diameters approximately 30−40 nm (prepared by electrochemical etching at 48 mA cm^{-2} for 35 s). After imprinting with a grating patterned stamp (area = 9 mm^2; grating pitch, Λ = 5 μm) at a force of $\sim$2kN as schematically illustrated in Figure 1, the imprinted regions are compressed to a thickness of approximately 615 nm while the other regions remain untouched. The mesoporous network accommodates the reduction in volume by bending and compressing pores together. In this case, the porous structure appears to be contiguous and unbroken. After imprinting, the sample was placed back in the electrochemical cell to determine if the densified porous network would prevent electrolyte infiltration and the etching of a second layer. Scanning electron microscope (SEM) imaging (Figure 2a) reveals that the etching of a second porous layer (20 mA cm^{-2}, 30 s) proceeded uniformly in both the printed and unprinted regions; the ethanolic HF etching solution readily infiltrated the entire imprinted pSi layer and reinitiated etching where the pores were previously terminated. This opens the possibility of fabricating devices through a multistep approach, where further electrochemical etching can be performed following DIPS. As an example of a device structure that would benefit from such a multistep process, we have fabricated a grating-coupled porous silicon waveguide sensor (Figure 2b); see the Supporting Information for details.

We next address the tunability of the imprinting process, focusing first on the imprint depth. From prior work on nanoindentation, we expect that the imprint depth depends primarily on the pressure applied to the stamp, the hardness of the material being imprinted, and the stamp geometry. Not surprisingly, we observed that the imprint depth of our stamp into porous materials scales with the applied pressure (Supporting Information Figure S1). What is perhaps more interesting is how porous nanomaterial properties, such as porosity, thickness, or conditioning methods (for example, oxidation in the case of pSi) affect the imprint depth through variations of material hardness. Atomic force microscopy (AFM) (Figure 2c,d) reveals that the imprint depth depends on all of these parameters; for a more detailed discussion, see the Supporting Information. By tuning the applied pressure and the film preparation conditions, we can easily achieve very precise, nanometer scale control over the imprint depth. We have also investigated imprinting porous structures to a depth that is a significant fraction of the original film thickness. This is particularly relevant for applications where a large aspect ratio is required. If we assume that volume reduction is accommodated primarily by a compression of the pores and a reduction of the void fraction, then the theoretical limit of the maximum imprintable film fraction should equal the original porosity of the film. We have come very close to this limit by imprinting a 1 μm thick pSi film with an initial porosity estimated at $\sim$80%, using an increased pressure (approximately 400 N/mm^2). Figure 2e shows that the porous silicon grating can be imprinted to a depth of 785 nm, very close to the theoretical limit of 800 nm. In this case, the imprinted region no longer resembles the compressed porous structure of Figure 2a, but rather resembles a crushed and densified film of broken silicon crystallites. The broken nature of the crushed film suggests that there no longer exists robust adhesion to the substrate, and indeed with ultrasonication the crushed region of pSi can be removed (Figure 2f). In this manner, imprinted structures can be produced with microscale vertical features and aspect ratios that exceed those of the stamp itself. We now turn to the variety of patterns that can be imprinted. Figure 3a,c reveals pSi and np-Au, respectively, after performing DIPS with a grating patterned stamp (area = 9 mm^2, Λ = 750 nm), which demonstrates the ability to pattern submicrometer features over large areas. The observed sidewall roughness confirms that the dimension of the pore diameter fundamentally limits the resolution of pattern transfer, as expected. DIPS is capable of patterning subwavelength optical structures of arbitrary nanoscale shapes, limited only by this resolution. This is demonstrated with the imprinting of text into pSi (in 3 μm size font) that contains curved features and details smaller than 100 nm (Figure 3b). A further demonstration of patterning curved features is included in Supporting Information Figure S2a. Alternatively, patterns can be easily scaled to produce larger, micrometer scale features and patterned arrays

dx.doi.org/10.1021/nl1028073 |*Nano Lett.* 2011, 11, 1857–1862

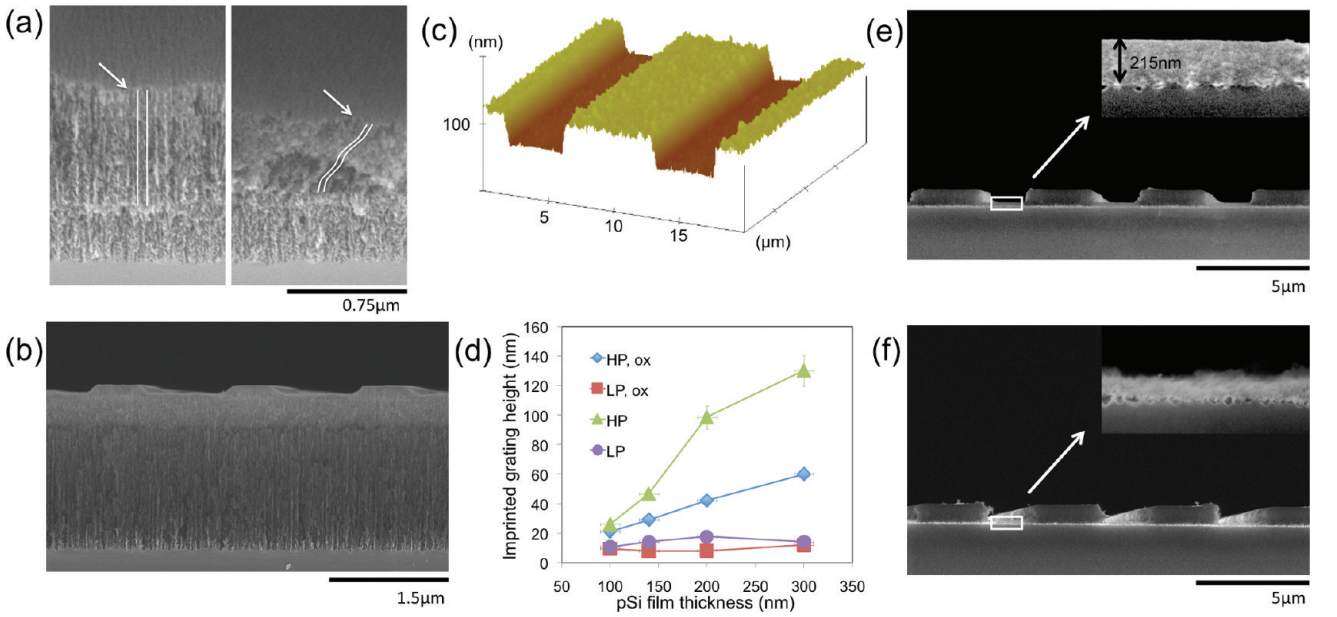

Figure 2. Characterization of vertical featuring of DIPS on pSi. (a) Cross-sectional SEM images (45° tilt) of unstamped and stamped regions of a 1 μm thick pSi film (the white arrows indicate highlighted typical pores). Following DIPS, a second layer could be uniformly etched in both regions. (b) SEM image of a grating coupled pSi waveguide fabricated with DIPS in a multistep process. (c) AFM height image of a typical pSi thin film after performing DIPS. (d) Variation of imprinted grating height for pSi thin films for various film thicknesses and preparation conditions. High-porosity (HP) and low-porosity (LP) films were electrochemically prepared at current densities of 80 and 5 mA cm^{-2}, respectively. Oxidation was performed at 500 °C for 5 min in air ambient. (e) SEM image of a pSi grating fabricated by imprinting a 1 μm thick HP film to a depth of 785 nm (the inset reveals a crushed pSi film remaining in the imprinted regions). (f) SEM image of a similarly prepared pSi grating where the crushed pSi region has been removed by ultrasonication (the inset reveals only the silicon substrate remains in the imprinted region).

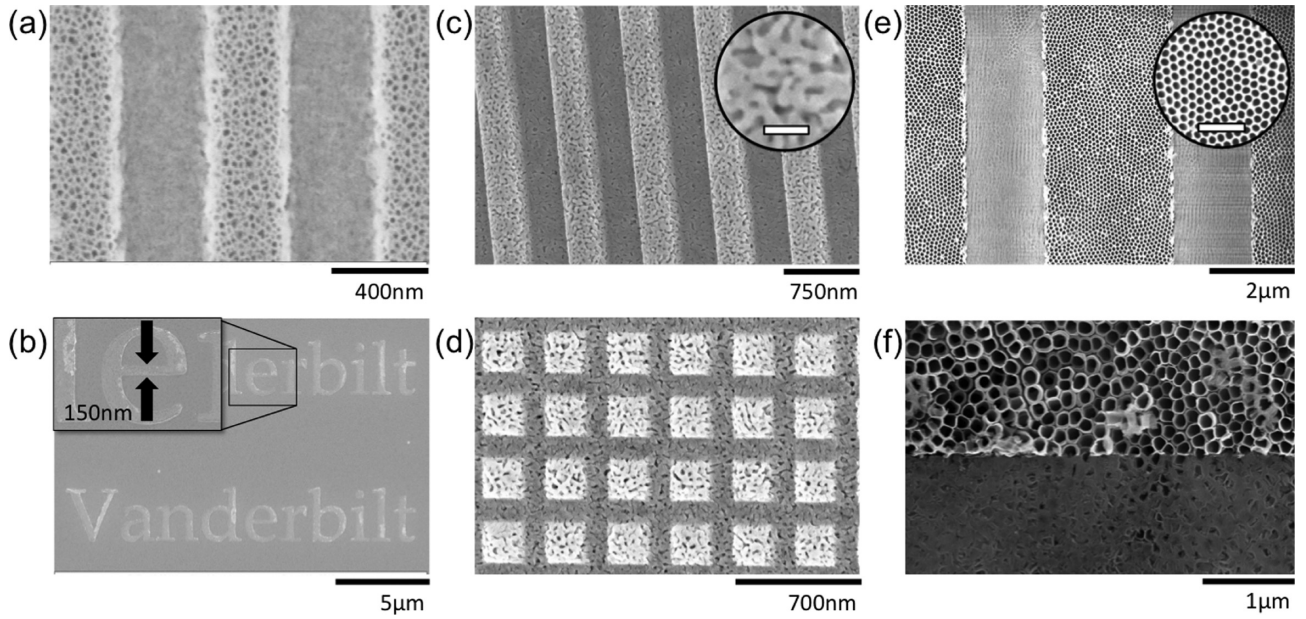

Figure 3. Top view SEM images of porous nanomaterials patterned with DIPS. (a) pSi grating (Λ = 750 nm) with submicrometer-sized features. The mean pore diameter is approximately 20−30 nm. (b) pSi imprinted with 3 μm font "Vanderbilt" text. (c) np-Au grating (Λ = 750 nm). Inset reveals the original pore morphology (scale bar = 100 nm). (d) np-Au square mesh produced by imprinting with a silicon grating (Λ = 350 nm), rotating 90° and imprinting again. (e) Imprinted pAl_2O_3 grating (Λ = 5 μm). Inset reveals the original pore morphology (scale bar =500 nm). (f) Imprinted and nonimprinted regions of a TiO_2-NTA.

(Supporting Information Figure S2b). Importantly, we note that we have observed no significant degradation of the stamps that have been reused more than 20 times nor have we observed any systematic reduction in the fidelity of imprints in porous substrates as a function of the number of times a stamp has been used; see Supporting Information and Figure S3a−c for details.

Figure 3d shows np-Au after imprinting with a grating patterned stamp (area = 9 mm^2, Λ = 350 nm), rotating 90°,

dx.doi.org/10.1021/nl1028073 |*Nano Lett.* 2011, 11, 1857–1862

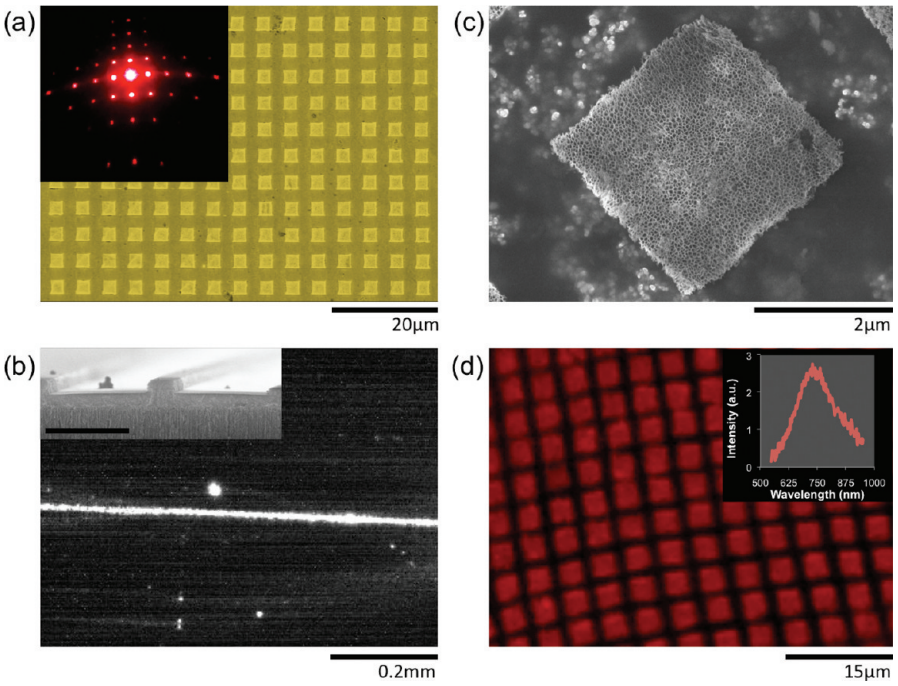

Figure 4. Demonstration of selected device structures fabricated by DIPS. (a) SEM image of a np-Au square diffraction grating ($\Lambda = 5\,\mu$m), produced in the same manner as in Figure 3d. Inset reveals the optical diffraction pattern ($\Lambda = 647$ nm) at approximately 15° from normal incidence. (b) Camera image (top view) of a DIPS-patterned pSi structure waveguiding near-infrared ($\Lambda = 1200-1700$ nm) light (the inset reveals a waveguide SEM cross-section, scale bar is 1 μm). (c) SEM image of a free-standing square pSi microparticle. (d) Confocal fluorescence micrograph of freestanding pSi microparticles on carbon tape (inset shows the photoluminescence spectra of an as-anodized pSi film, excitation $\Lambda = 488$ nm).

and imprinting again. This demonstrates that "step and print" structures can be constructed, where a stamp is shifted or rotated multiple times between imprints to achieve structures more complex than that of the stamp itself. The resulting structure here is a nanoscale square mesh of np-Au. To our knowledge, this demonstrates a patterning resolution never before achieved on np-Au. On the basis of these results, we expect that DIPS could be employed to realize a new class of low-cost plasmonic devices employing np-Au.[20,32] DIPS has also been successfully used to imprint hexagonally ordered pAl_2O_3 (Figure 3e) as well as disordered pAl_2O_3 (Supporting Information Figure S4). Figure 3f shows the imprinted and nonimprinted regions of a TiO_2-NTA and reveals results similar to those obtained with other porous nanomaterials (also see Supporting Information Figure S5). These results indicate that a host of porous materials can be imprinted using DIPS with excellent pattern reproduction and large area uniformity.

To suggest the variety of applications that could be enabled by DIPS, we have fabricated several sample structures (Figure 4). First, we show that appropriately patterned DIPS structures can be readily used as optical diffraction gratings. Figure 4a reveals a square diffraction grating fabricated on np-Au on a glass substrate. A clear and distinct diffraction pattern appears due to the large spatial uniformity of the imprinted microscale pattern. This demonstrates that DIPS is capable of patterning macro- to microscale arrays, an important class of structures on porous nanomaterials. The fabrication of diffraction gratings in porous materials is particularly relevant to sensing applications, where the presence of analytes in the porous matrix modifies the effective refractive index of the grating, leading to significant changes in the diffraction signature. We have recently demonstrated this phenomenon for label-free sensing of small molecules using a micrometer-scale one-dimensional porous dielectric grating,[12] and for significantly enhanced SERS sensing using a submicrometer-scale two-dimensional porous metal grating.[32] Porous diffraction gratings could also be utilized to couple light into dielectric waveguides (as in Figure 2b) or launch surface plasmons in metallic films. Furthermore, grating structures are of particular interest in photovoltaic applications, owing to their ability to couple light into guided modes of thin-film devices for light harvesting.[33]

As a second example, we report the ability to fabricate 3D waveguides (Figure 4b) utilizing DIPS on pSi in a multistep process similar to that previously described for the grating coupled 2D waveguide (Figure 2b). Horizontal confinement of light (coplanar direction) is achieved by imprinting trenches into a ~450 nm thickness medium porosity (~67%) pSi film prepared at a current density of 20 mA cm^{-2}. Subsequent etching of a 1.8 μm thick high porosity (~80%) pSi cladding layer (80 mA cm^{-2}) produces the vertical confinement required for waveguiding. An advantage of utilizing photonic structures constructed from porous nanomaterials is the ability to infiltrate various species into the porous network that can then be used in switching, sensing, or light emission applications.[34−36] Note that with this pSi waveguide example, we demonstrate that DIPS is well equipped for patterning submicrometer and nanoscale structures.

In Figure 4c,d, we present the ability to fabricate microscale structures, in particular freestanding pSi microparticles, using DIPS. The fabrication follows a procedure similar to that described above (Figure 3d) with some modifications. When a stamp is imprinted all the way into pSi with the entire stamp surface brought into contact with the substrate, a new and interesting stamping regime occurs. We refer to it as "overstamping", to

dx.doi.org/10.1021/nl1028073 |*Nano Lett.* 2011, 11, 1857–1862

distinguish it from the previous examples we have presented. Overstamping affords the ability to selectively weaken the base of the porous nanostructure (Supporting Information Figure S6). In this manner, patterned structures can be easily detached from the substrate. This can be done by using the combination of frictional and electrostatic forces that exist between the stamp and the imprinted structure (Supporting Information Figure S7) by performing ultrasonication in an aqueous solution or by simply applying and removing an adhesive such as carbon tape (Figure 4c,d). These pSi microparticles exhibit excellent size uniformity and can be readily placed in solution. Other particle geometries could also be realized on both the micro- and nanoscale by simply changing the geometry of the applied stamp. Selected particles can exhibit highly desirable traits for use in vivo that include efficient loading of therapeutics or imaging contrast agents, distinctive photoluminescence or other signatures, and biodegradability.[6−8] In Figure 4d, we further demonstrate that these pSi microparticles maintain their intrinsic photoluminescence properties. In addition to particular interest for in vivo applications, we note that the design of isolated porous particles is also of growing interest for Si-based Li-ion battery anodes, which are particularly attractive for their large specific capacity, low volume, lightweight, and potentially low cost.[19]

In summary, DIPS offers an exciting and straightforward approach for realizing a large variety of important structures based on a wide class of porous nanomaterials. While our implementation of the DIPS process currently utilizes only a normal force (i.e., perpendicular to the plane of the stamp), a lateral or shear force component could also be added to produce an even wider variety of interesting imprinted topographies. We have demonstrated using DIPS for the fabrication of three classes of structures particularly relevant to porous nanomaterials including (i) macro- to microscale arrays, (ii) microscale structures, and (iii) submicrometer to nanoscale elements. The DIPS process enables the fabrication of these structures with an unprecedented combination of fast throughput, low cost, and high resolution. As a result, DIPS enhances both the commercialization potential and accessibility of nanostructured materials and devices. Moreover, we have demonstrated the use of DIPS on insulating, semiconducting, and metallic porous materials. DIPS circumvents the need for lithography, or masking materials and etch chemistries, that form the usual paradigms for the fabrication of structures from porous media. Thus DIPS may open a new class of low-cost technologies utilizing porous materials.

Preparation of Porous Nanomaterials. pSi samples were prepared by electrochemical etching of a boron doped p+ type Si(100) with a resistivity of 0.01−0.02 Ω cm and a thickness of 475−550 μm (University Wafer) in a mixture of 49% hydrofluoric acid (HF)/ethanol mixture with a ratio of 3:7 (v/v). np-Au samples were prepared from a ∼1.5 × 1.5 cm sheet of 100 nm thick Monarch 12 karat white gold (fineartstore.com) that was dealloyed by floating on concentrated nitric acid for 15 min followed by mounting on substrate supports, as reported elsewhere.[24] Hexagonally ordered pAl_2O_3 was prepared by anodization of high purity 100 μm thick Al foil (99.99%, Sigma Aldrich) in 0.3 M oxalic acid electrolyte according to the literature.[1] The pores were subsequently opened in a bath of phosphoric acid (5 wt %) for 90 min. TiO_2-NTAs were prepared from 0.25 mm thick Ti foil (99.7%, Sigma Aldrich), cut into 2 × 2 cm squares that were first sonicated in isoproponal and then acetone, each for 10 min. Samples were then anodized at 80 V for 5−18 h in a two-electrode configuration utilizing an electrolyte solution of NH_4F (0.3% by weight) and water (0.1% by volume) in ethylene glycol and subsequently annealed at 450 °C for 3 h with a 3.5 h ramp up/down time.

Stamp Preparation and Imprinting. Silicon stamps were prepared from the same wafers used to prepare the pSi samples (described above). Standard photolithography and reactive ion etching were used to pattern the microscale (Λ = 5, 10 μm) grating stamps. All other stamp patterns were defined by electron-beam lithography followed by (i) electron-beam evaporation of a 10 nm Cr mask layer, (ii) lift-off in acetone, and (iii) subsequent reactive ion etching to a depth of approximately 0.5 μm (except for the submicrometer period gratings, which skipped steps i and ii). Imprinting was performed with a Tinius Olsen Super L 60K universal testing machine configured to apply a flat metallic plate onto the backside of the stamp, which was fixed face down on the porous nanomaterial with single-sided Scotch Tape. After bringing the plate into contact with the backside of the stamp, a computer-controlled force was delivered and sustained for less than 1s.

■ ASSOCIATED CONTENT

Supporting Information. Detailed methods, discussion, and figures. This material is available free of charge via the Internet at http://pubs.acs.org.

■ AUTHOR INFORMATION

Corresponding Author
*E-mail: sharon.weiss@vanderbilt.edu.

■ ACKNOWLEDGMENT

This work was supported in part by the Army Research Office Grant W911NF-09-1-0101. SEM and AFM were performed at the Vanderbilt Institute of Nanoscale Science and Engineering. Photolithography, electron-beam-lithography (EBL), and reactive ion etching (RIE) of the silicon stamps were performed at the Center for Nanophase Materials Sciences, which is sponsored at Oak Ridge National Laboratory by the Division of Scientific User Facilities, U.S. Department of Energy. The authors gratefully thank F. Sanchez and C. Gay for assistance with the stamping tool, D. Li and S. Vajandar for providing hexagonally ordered pAl_2O_3, K. Jennings and P. Ciesielski for providing np-Au, S. Rosenthal and S. Rosson for providing TiO_2-NTAs, C. Kang for assistance with EBL and RIE, X. Wei for assistance with the grating coupled waveguide, and S. Wells for confocal fluorescence microscope imaging. J.D.R. acknowledges support from an NSF Graduate Research Fellowship. M.L. acknowledges CNISM funding through the INNESCO project. J.E.S. acknowledges support from The National Sciences and Engineering Research Council of Canada and the Ontario Centre of Excellence program.

■ REFERENCES

(1) Li, A. P.; Müller, F.; Birner, A.; Nielsch, K.; Gösele, U. *J. Appl. Phys.* **1998**, *84*, 6023.
(2) Ding, Y.; Kim, Y.-J.; Erlebacher, J. *Adv. Mater.* **2004**, *16*, 1897.
(3) Kasuga, T.; Hiramatsu, M.; Hoson, A.; Sekino, T.; Niihara, K. *Langmuir* **1998**, *14*, 3160.
(4) Smith, R. L.; Collins, S. D. *J. Appl. Phys.* **1992**, *71*, R1.

(5) Walcarius, A.; Sibottier, E.; Etienne, E.; Ghanbaja, J. *Nat. Mater.* **2007**, *6*, 602.
(6) Tasciotti, E.; Liu, X.; Bhavane, R.; Plant, K.; Leonard, A. D.; Price, B. K.; Cheng, M. M.-C.; Decuzzi, P.; Tour, J. M.; Robertson, F.; Ferrari, M. *Nat. Nanotechnol.* **2008**, *3*, 151.
(7) Park, J.-H.; Gu, L.; Maltzahn, G.; von; Ruoslahti, E.; Bhatia, S. N.; Sailor, M. J. *Nat. Mater.* **2009**, *8*, 331.
(8) Horcajada, P.; Chalati, T.; Serre, C.; Gillet, B.; Sebrie, C.; Baati, T.; Eubank, J. F.; Heurtaux, D.; Clayette, P.; Kreuz, C.; Chang, J.-S.; Hwang, Y. K.; Marsaud, V.; Bories, P.-N.; Cynober, L.; Gil, S.; Férey, G.; Couvreur, P.; Gref, R. *Nat. Mater.* **2010**, *9*, 172.
(9) Cunin, F.; Schmedake, T. A.; Link, J. R.; Li, Y. Y.; Koh, J.; Bhatia, S. N.; Sailor, M. J. *Nat. Mater.* **2002**, *1*, 39.
(10) Varghese, O. K.; Gong, D.; Paulose, M.; Ong, K. G.; Dickey, E. C.; Grimes, C. A. *Adv. Mater.* **2003**, *15*, 624.
(11) Alvarez, S. D.; Li, C.-P.; Chiang, C. E.; Schuller, I. K.; Sailor, M. J. *ACS Nano* **2009**, *3*, 3301.
(12) Ryckman, J. D.; Liscidini, M.; Sipe, J. E.; Weiss, S. M. *Appl. Phys. Lett.* **2010**, *96*, 171103.
(13) Rolison, D. R. *Science* **2003**, *299*, 1698.
(14) Wittstock, A.; Zielasek, V.; Biener, J.; Friend, C. M.; Bäumer, M. *Science* **2010**, *327*, 319.
(15) Adachi, M.; Murata, Y.; Harada, M.; Yoshikawa, S. *Chem. Lett.* **2000**, 942.
(16) Sun, W.; Puzas, J. E.; Sheu, T.-J.; Liu, X.; Fauchet, P. M. *Adv. Mater.* **2007**, *19*, 921.
(17) Low, S. P.; Williams, K.; Canham, L. T.; Voelcker, N. H. *Biomaterials* **2006**, *27*, 4538.
(18) Chan, C. K.; Peng, H.; Liu, G.; McIlwrath, K.; Zhang, X. F.; Huggins, R. A.; Cui, Y. *Nat. Nanotechnol.* **2008**, *3*, 31.
(19) Magasinski, A.; Dixon, P.; Hertzberg, B.; Kvit, A.; Ayala, J.; Yushin, G. *Nat. Mater.* **2010**, *9*, 353.
(20) Biener, J.; Nyce, G. W.; Hodge, A. M.; Biener, M. M.; Hamza, A. V.; Maier, S. A. *Adv. Mater.* **2008**, *20*, 1211.
(21) Iyer, S. S.; Xie, Y.-H. *Science* **1993**, *260*, 40.
(22) Hirschman, K. D.; Tsybeskov, L.; Duttagupta, S. P.; Fauchet, P. M. *Nature* **1996**, *384*, 338.
(23) Varghese, O. K.; Paulose, M.; Grimes, C. A. *Nat. Nanotechnol.* **2009**, *4*, 592.
(24) Ciesielski, P. N.; Scott, A. M.; Faulkner, C. J.; Berron, B. J.; Cliffel, D. E.; Jennings, G. K. *ACS Nano* **2008**, *2*, 2465.
(25) Ito, S.; Zakeeruddin, S. M.; Comte, P.; Liska, P.; Kuang, D.; Grätzel, M. *Nat. Photonics* **2008**, *2*, 693.
(26) Chou, S. Y.; Krauss, P. R.; Renstrom, P. J. *J. Vac. Sci. Technol., B* **1996**, *14*, 4129.
(27) Zankovych, S.; Hoffman, T.; Seekamp, J.; Bruch, J.-U.; Sotomayor Torres, C. M. *Nanotechnology* **2001**, *12*, 91.
(28) Kumar, G.; Tang, H.; Schroers, J. *Nature* **2009**, *457*, 868.
(29) Ji, J.; Li, X.; Canham, L. T.; Coffer, J. L. *Adv. Mater.* **2002**, *14*, 41.
(30) Chou, S. Y.; Keimel, C.; Gu, J. *Nature* **2002**, *417*, 835.
(31) Gong, J.; Lipomi, D. J.; Deng, J.; Nie, Z.; Chen, X.; Randall, N. X.; Nair, R.; Whitesides, G. M. *Nano Lett.* **2010**, *10*, 2702.
(32) Jiao, Y.; Ryckman, J. D.; Ciesielski, P. N.; Jennings, G. K.; Weiss, S. M. To be submitted for publication.
(33) Zanotto, S.; Liscidini, M.; Andreani, L. C. *Opt. Express* **2010**, *18*, 4260.
(34) Wei, X.; Kang, C. K.; Liscidini, M.; Rong, G.; Retterer, S. T.; Patrini, M.; Sipe, J. E.; Weiss, S. M. *J. Appl. Phys.* **2008**, *102*, 123113.
(35) Weiss, S. M.; Ouyang, H. M.; Zhang, J. D.; Fauchet, P. M. *Opt. Express* **2005**, *13*, 1090.
(36) Weiss, S. M.; Zhang, J.; Fauchet, P. M.; Seregin, V. V.; Coffer, J. L. *Appl. Phys. Lett.* **2007**, *90*, No. 031112.